

Topological quantum field theory and polynomial identities for graphs on the torus

Paul Fendley and Vyacheslav Krushkal

Abstract. We establish a relation between the trace evaluation in $\mathrm{SO}(3)$ topological quantum field theory and evaluations of a topological Tutte polynomial. As an application, a generalization of the Tutte golden identity is proved for graphs on the torus.

1. Introduction

The Witten–Reshetikhin–Turaev topological quantum field theory (TQFT) associates invariants to ribbon graphs in 3-manifolds. A part of this theory is an invariant of graphs on surfaces: given a graph $G \subset \Sigma$, the *trace evaluation* is the invariant associated to the embedding $G \subset \Sigma \times \{*\} \subset \Sigma \times S^1$. We study the trace evaluation for $\mathrm{SO}(3)$ TQFTs.

For *planar* graphs, the $\mathrm{SO}(3)$ quantum evaluation is known to equal the flow polynomial $F_G(Q)$, or equivalently the chromatic polynomial $\chi_{G^*}(Q)$ of the dual graph. The parameter Q is related to level of the TQFT, as reviewed in Section 2. In [11] we showed that this quantum-topological approach gives a conceptually and calculationally useful framework for analyzing the relations satisfied by the chromatic and flow polynomials of planar graphs. In particular, we gave a proof in this setting of the Tutte golden identity [25]: given a planar triangulation T ,

$$\chi_T(\phi + 2) = (\phi + 2)\phi^{3V(T)-10}(\chi_T(\phi + 1))^2, \quad (1.1)$$

where $V(T)$ is the number of vertices of the triangulation, and the graph parameters both involve the golden ratio $\phi = \frac{1+\sqrt{5}}{2}$. The dual formulation in terms of the flow polynomial states that for a planar cubic graph G , $F_G(\phi + 2) = \phi^E(F_G(\phi + 1))^2$. In [11] we also showed that the golden identity may be thought of as a consequence of level-rank duality between the $\mathrm{SO}(3)_4$ and the $\mathrm{SO}(4)_3$ TQFTs, and the isomorphism

2020 Mathematics Subject Classification. Primary 57K16; Secondary 57M15, 05C31, 82B20.

Keywords. Topological quantum field theory, graphs on surfaces, topological Tutte polynomial, the Tutte golden identity.

$\mathfrak{so}(4) \cong \mathfrak{so}(3) \times \mathfrak{so}(3)$. (Consequences of SO level-rank duality for link polynomials have also been studied in [21].)

The main purpose of this paper is to formulate an extension of the results on TQFT and polynomial invariants to graphs on the torus; in particular we prove a generalization of the golden identity. Some of the motivation for this work has its origins in lattice models in statistical mechanics, where it has long been known (see, e.g., [10, 23]) that when deriving identities for partition functions on the torus, one must typically sum over “twisted” sectors. Twisted sectors are more complicated analogues of the spin structures (cf. [7]) familiar in field theories involving fermions. Such sectors are described naturally in TQFT, as for example can be seen in the study of lattice topological defects [1, 2]. We show how the golden identity is generalised to the torus precisely by considering such sums over analogous sectors. In a forthcoming paper [13] we will elaborate further on the connections to statistical mechanics, in particular on the relation with the Pasquier height model [23].

The chromatic and flow polynomials are 1-variable specializations of the Tutte polynomial, known in statistical mechanics as the partition function of the Potts model. Relations between the SO(3) quantum evaluation of planar graphs, the chromatic and flow polynomial, and the Potts model are discussed in detail in [12]. From the TQFT perspective, the case of graphs embedded in the plane (or equivalently in the 2-sphere S^2) is very special in that the TQFT vector space associated to S^2 is \mathbb{C} . For surfaces Σ of higher genus, they are vector spaces (of dimension given by the Verlinde formula) which are part of the rich structure given by the $(2 + 1)$ -dimensional TQFT. Multi-curves, and more generally graphs embedded in Σ , act as “curve operators” on the TQFT vector space, and our goal is to analyze the trace of these operators.

For the SO(3) TQFT, this invariant of graphs on surfaces satisfies the contraction-deletion rule, familiar from the study of the Tutte polynomial. A non-trivial feature on surfaces of higher genus is that the “loop value” depends on whether the loop is trivial (bounds a disk) in the surface, or whether it wraps non-trivially around the surface. In the latter case, the invariant is not multiplicative under adding/removing a loop, as opposed to the planar case. This behavior is familiar in generalizations of the Tutte polynomial which encode the topological information of the graph embedding in a surface. The study of such “topological” graph polynomials was pioneered by Bollobás and Riordan [6]; a more general version was introduced in [18]. To express the SO(3) trace evaluation for graphs on the torus we need a further extension of the polynomial, defined in Section 3. In Theorem 4.4 we show that the quantum invariant equals a sum of values of the polynomial, where the sum is parametrized by labels corresponding to the TQFT level. Here individual summands (evaluations of the topological Tutte polynomial) correspond to TQFT sectors.

The identity (1.1) for the chromatic polynomial and its analogue for the flow polynomial in general do *not* hold for non-planar graphs. In fact, it is conjectured [3] that

the golden identity for the flow polynomial characterizes planarity of cubic graphs. Our result (Theorem 5.1) involves invariants of graphs derived from TQFT, or equivalently evaluations of graph polynomials, and it recovers the original Tutte’s identity for planar graphs.

A different “quantum” version of the golden identity, for the Yamada polynomial of ribbon cubic graphs in \mathbb{R}^3 , was established in [4]. It is an extension of the Tutte identity from the flow polynomial of planar graphs to the Yamada polynomial of spatial graphs, which may be thought of as elements of the skein module of S^2 (isomorphic to \mathbb{C}). Our result manifestly involves graphs on the torus and the elements they represent in the associated TQFT vector spaces. We expect that an extension of our results holds on surfaces of genus > 1 as well, although computational details on surfaces of higher genus are substantially more involved.

To date, the study of topological Tutte polynomials of graphs on surfaces has been carried out primarily in the context of topological combinatorics. While there are applications to quantum invariants of links (cf. [8, 20]) and to noncommutative quantum field theory [17], to our knowledge the results of this paper provide the first direct relation between TQFT and evaluations of graph polynomials on surfaces.

We emphasize that the relation between evaluations of the topological flow polynomial and the TQFT trace, the main result of this paper, is specific to values of the graph polynomial corresponding to roots of unity. This is a new feature on the torus – recall that in the planar case the $SO(3)$ quantum evaluation (or “loop evaluation,” cf. [11, Lemma 2.5]) of planar graphs holds for *any* value of the parameter.

It is worth noting that the results of this paper apply to a topological flow polynomial for graphs in a fixed surface, the torus (see [18] and Section 3 below). This context is different from that of the Bollobás–Riordan polynomial [6] of ribbon graphs: the underlying surface in the ribbon graph setting (and the topological invariants associated to it) depend on a specific graph, and in particular the surface may change when the contraction-deletion rule is applied. Thus, our results do not have an immediate analogue for the Bollobás–Riordan polynomial.

After briefly reviewing background information on TQFT in Section 2, we define the relevant topological Tutte polynomial for graphs on the torus in Section 3. The relation between TQFT trace and evaluation of the graph polynomial is stated and proved in Section 4. The generalization of the golden identity for graphs on the torus is established in Section 5.

2. Background on TQFT

We start with a brief introduction to the Temperley–Lieb algebra and the Jones–Wenzl projectors [15, 28]; the reader is referred to [11] for a more detailed discussion, and to [16] for an introduction to the calculus of quantum spin networks.

The Temperley–Lieb algebra in degree n , TL_n , is an algebra over $\mathbb{C}[d]$ generated by $1, E_1, \dots, E_{n-1}$ with the relations [24]

$$E_i^2 = E_i, \quad E_i E_{i\pm 1} E_i = \frac{1}{d^2} E_i, \quad E_i E_j = E_j E_i \quad \text{for } |i - j| > 1. \quad (2.1)$$

The construction of TQFTs relies on setting the indeterminate d to a special value $d = 2 \cos \frac{\pi}{l+2}$ where l is a positive integer called the level.

The elements of TL_n may be represented pictorially as linear combinations of 1-dimensional submanifolds in a rectangle R , where the submanifolds are considered equivalent if they are isotopic relative to the boundary. Each submanifold meets both the top and the bottom of the rectangle in exactly n points. The multiplication then corresponds to vertical stacking of rectangles. The generators of TL_3 are illustrated in Figure 1.

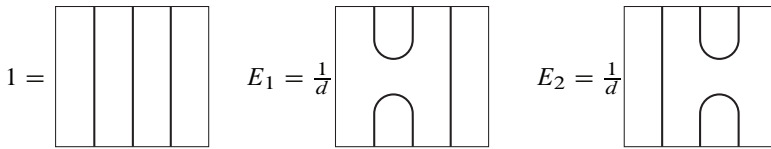


Figure 1. Generators of TL_3 .

In this setting, the relation $E_i^2 = E_i$ implies that the element in TL_n corresponding to a picture in R with a simple closed curve C is equivalent to the element with the curve C deleted and multiplied by d .

To fix the notation, recall the definition of quantum integers $[n]$, and the evaluation of the n -colored unknot, Δ_n :

$$[n] = \frac{A^{2n} - A^{-2n}}{A^2 - A^{-2}}, \quad \Delta_n = [n + 1].$$

We will interchangeably use the parameters q, A , as well as the loop value d and a graph parameter Q , related as follows:

$$q = A^4, \quad d = A^2 + A^{-2}, \quad Q = d^2. \quad (2.2)$$

The Jones–Wenzl projectors $p_n \in TL_n$ are certain idempotent elements of the Temperley–Lieb algebra, underlying the construction of $SU(2)$ topological quantum

field theories and quantum spin networks. The second Jones–Wenzl projector $p_2 = 1 - E_1$ is illustrated on the left in equation (2.4). A recursive formula [16] giving the rest is

$$p_n = p_{n-1} - \frac{d \Delta_{n-2}}{\Delta_{n-1}} p_{n-1} E_{n-1} p_{n-1}. \tag{2.3}$$

This recursion relation is illustrated in Figure 2. A defining feature of the projectors is that they are “killed by turnbacks,” that is $E_i p_n = p_n E_i = 0$ for each $i = 1, \dots, n - 1$. At values corresponding to q a root of unity: specifically $d = 2 \cos(\theta)$, $\theta = \pi j/n + 1$, the trace of p_n also equals zero. In other words, for these values of the parameter p_n is in the *trace radical* of the Temperley–Lieb algebra; for more details see [11, Sections 2 and 5.2]. The 4th projector p_4 plays a crucial role in the proof of the Tutte golden identity, as explained in [11] and in Section 5.1 of this paper.

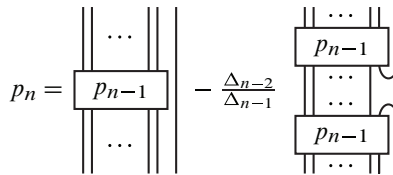


Figure 2. A recursive formula for the Jones–Wenzl projectors.

2.1. SU(2) TQFTs

We use the construction of SU(2) Witten–Reshetikhin–Turaev TQFTs, given in [5]. Given a closed orientable surface Σ , the SU(2), level $r - 2$ TQFT vector space will be denoted $V_r(\Sigma)$, where $A = e^{2\pi i/4r}$. (Note that in the TQFT literature the notation V_{2r} is sometimes used instead. Also note that, in the physics literature, labels are often divided by 2 and called “spin,” so that odd and even labels correspond to half-integer and integer spins respectively.)

The main focus of this paper is on the torus case, $\Sigma = \mathbb{T}$, and in this case the notation $V_r := V_r(\mathbb{T})$ will be used throughout the paper. Consider \mathbb{T} as the boundary of the solid torus H . V_r has a basis $\{e_0, \dots, e_{r-2}\}$, where e_j corresponds to the core curve of H , labeled by the j -th projector p_j . This basis will be used in the evaluation of the trace in Section 4.1.

The discussion in the rest of this section applies to surfaces Σ of any genus. A curve γ in Σ acts as a linear operator on $V_r(\Sigma)$, so associated to γ is an element of $V_r^*(\Sigma) \otimes V_r(\Sigma)$. Given a graph $G \subset \Sigma$, we consider it as an SU(2) quantum spin network in Σ by turning each edge into a “double line.” Namely, as in [11] we label edges by the second Jones–Wenzl projector, up to an overall normalization. Concretely, each

edge e of G is replaced with a linear combination of curves as indicated in (2.4), and the curves are connected without crossings on the surface near each vertex.

$$e \xrightarrow{\Phi} \left(\text{two parallel vertical lines with a small circle between them} \right) = \left(\text{two parallel vertical lines} \right) - \frac{1}{d} \left(\text{two U-shaped curves} \right) \quad \text{and} \quad \left(\text{X-shaped crossing} \right) \xrightarrow{\Phi} d \cdot \left(\text{four curves meeting at a central point with small circles} \right) \quad (2.4)$$

In this map, a factor $d^{(k-2)/2}$ is associated to each k -valent vertex, so that for example the 4-valent vertex in (2.4) is multiplied by d . The overall factor for a graph G is the product of the factors $d^{(k(V)-2)/2}$ over all vertices V of G . Therefore, the total exponent equals half the sum of valencies over all vertices, minus the number of vertices, i.e., minus the Euler characteristic of G . (This count does not involve faces – so this is the Euler characteristic of the graph G , and not of the underlying surface Σ .) Using this map Φ , the graph is mapped to a linear combination of multicurves in the surface Σ . We thus may consider graphs G on the torus as elements $\Phi(G) \in \text{Hom}(V_r, V_r)$.

To illustrate the calculation of $\Phi(G)$, consider a simple example where the graph G consists of a single vertex and a single edge which forms a non-trivial loop on the torus, as shown in Figure 3. (Calculations for more general graphs on the torus are given in Sections 4.1 and 4.3.)

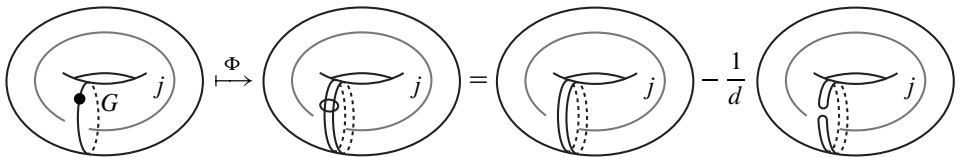


Figure 3. Example of an evaluation of Φ .

Note that the calculation in Figure 3 is specific to the chosen basis. That is, in this calculation the solid torus bounded by \mathbb{T} is chosen so that the loop given by G bounds a compression disk in it; in particular, the core of the solid torus intersects this disk in a single point. Other loops on the torus will have different evaluations with respect to this basis. The focus in this paper (explained in more detail in Section 4) is on the trace of $\Phi(G)$ which of course is basis independent.

Applying Φ in this example amounts to replacing the edge of the graph with the 2nd projector, which equals the linear combination of the two terms shown in the figure. The first term has two parallel, non-trivial 1-labeled (or “spin 1/2”) loops, while the last term has a single trivial loop on the torus.

To determine the action of non-trivial loops, recall a basic calculation for the colored Hopf link

$$\begin{array}{c} | \\ m \text{---} \bigcirc \text{---} | \\ | \\ n \end{array} = \frac{[(m+1)(n+1)]}{[n+1]} \begin{array}{c} | \\ | \\ | \\ n \end{array} \tag{2.5}$$

Thus, $\Phi(G)$ with respect to the basis $\{e_0, \dots, e_{r-2}\}$, of V_r is given by the diagonal matrix with the (j, j) -th entry given by $\left(\frac{[2(j+1)]}{[j+1]}\right)^2 - 1$. It is worth noting that in this special case formula (2.5) could be applied directly to G , considered as a 2-labelled loop, giving the diagonal entry $\frac{[3(j+1)]}{[j+1]}$ which matches the calculation above using Φ .

Returning to the general discussion of graphs on the torus, given a graph $G \subset \mathbb{T}$, consider the following local relations (1)–(3), illustrated in Figures 4 and 5.

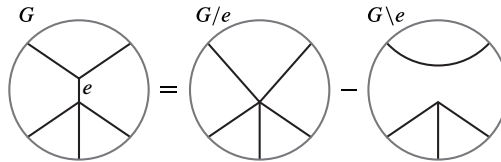


Figure 4. Relation (1).

(1) If e is an edge of a graph G which is not a loop, then $G = G/e - G \setminus e$, as illustrated in Figure 4.

(2) If G contains an edge e which is a trivial loop, that is a trivial loop that bounds a disk in \mathbb{T} , then $G = (Q - 1) G \setminus e$, as in Figure 5. (In particular, this relation applies if e is a trivial loop not connected to the rest of the graph.)

(3) If G contains a 1-valent vertex as in Figure 5, then $G = 0$.

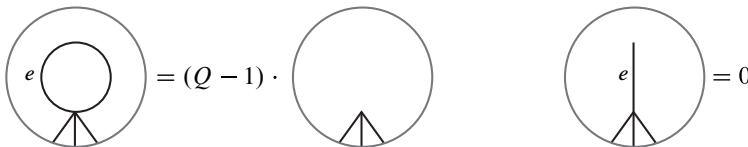


Figure 5. Relations (2) and (3).

Replacing the edge labeled e in each figure with the linear combination of curves, defined by the second JW projector, one checks that the relations (1)–(3) hold for $\Phi(G)$ in $\text{Hom}(V_r, V_r)$, where the parameters A, Q are related as in (2.2), and the value of A in the definition of V_r is $e^{2\pi i/4r}$.

Remark 2.2. In the planar case, the map gives a homomorphism from the *chromatic algebra* \mathcal{C}_n^Q , defined in [11], to the Temperley–Lieb algebra TL_{2n}^d , with the parameters related by $Q = d^2$. This map is used to show [11, Lemma 2.5] that for planar graphs G , up to a normalization the quantum evaluation equals the flow polynomial of G or equivalently the chromatic polynomial of the dual graph G^* . Indeed, relations (1)–(3) are sufficient for evaluating any graph *in the plane*, and these relations are precisely the defining relation for the chromatic polynomial (of the dual graph). On the torus, or any other surface of higher genus, the “evaluation” is not an element of \mathbb{C} but rather an element of the higher-dimensional TQFT vector space $\text{Hom}(V_r, V_r)$.

A crucial feature underlying the construction of TQFTs is that for each r , *in addition to* (1)–(3) there is another local relation corresponding to the vanishing of the corresponding Jones–Wenzl projector. For example, consider the case $r = 5$, important in the proof of the golden identity below. In this case, graphs $G \subset \Sigma$, considered as elements of the vector space $\text{Hom}(V_5(\Sigma), V_5(\Sigma))$, satisfy the local relation in (2.6).

$$\phi \begin{array}{c} \text{---} \text{---} \\ \diagup \quad \diagdown \\ \text{---} \text{---} \\ G_X \end{array} = \begin{array}{c} \text{---} \text{---} \\ \text{---} \text{---} \\ G_I \end{array} + \begin{array}{c} \text{---} \text{---} \\ \text{---} \text{---} \\ G_E \end{array} \tag{2.6}$$

This relation (discovered in the setting of the chromatic polynomial of planar graphs by Tutte [26]) corresponds to the 4th JW projector, see [11, Section 2] for more details.

Remark 2.3. In fact, the Turaev–Viro $SU(2)$ TQFT associated to a surface Σ , isomorphic to $\text{Hom}(V_r(\Sigma), V_r(\Sigma))$, can be defined as the vector space spanned by multicurves on Σ , modulo the local relations given by “ d -isotopy” and the vanishing of the JW projector. (See [14, Theorem 3.14 and Section 7.2].) The $SO(3)$ theory may be built by considering the “even labels” subspace spanned by graphs modulo relations (1)–(3) above, and the JW projector.

3. Polynomial invariants of graphs on surfaces

Let H be a graph embedded in the torus \mathbb{T} . Let $n(H)$ denote the nullity of H , that is the rank of the first homology group $H_1(H; \mathbb{Z})$. The rank¹ $r(H \subset \mathbb{T})$ of the image of the map $i_*: H_1(H; \mathbb{Z}) \rightarrow H_1(\mathbb{T}; \mathbb{Z}) \cong \mathbb{Z}^2$, induced by the inclusion $H \subset \mathbb{T}$, is either

¹Note that this topological rank notion reflects information about the embedding of the graph in the torus, and it is different from other notions of rank considered in graph theory.

0, 1 or 2. Consider the following homological invariants:

$$s(H) := \begin{cases} 1 & \text{if } r(H \subset \mathbb{T}) = 2 \text{ (i.e., } H_1(H) \rightarrow H_1(\mathbb{T}) \text{ is surjective),} \\ 0 & \text{otherwise.} \end{cases} \tag{3.1}$$

$$s^\perp(H) := \begin{cases} 1 & \text{if } r(H \subset \mathbb{T}) = 0 \text{ (i.e., } H_1(H) \rightarrow H_1(\mathbb{T}) \text{ is the zero map),} \\ 0 & \text{otherwise.} \end{cases} \tag{3.2}$$

Let $c(H)$ be the number of rank 0 connected components of H , that is the number of connected components $H^{(i)}$ such that $r(H^{(i)} \subset \mathbb{T}) = 0$.

In case $r(H \subset \mathbb{T}) = 1$, let $\bar{c}(H)$ be the number of “essential” components of H , i.e., the number of components $H^{(i)}$ such that $H_1(H^{(i)}) \rightarrow H_1(\mathbb{T})$ is non-trivial. (Note that for each such component, the image of the map on homology is the same rank 1 subgroup of $H_1(\mathbb{T})$.) If $r(H \subset \mathbb{T})$ is 0 or 2, $\bar{c}(H)$ is defined to be zero.

Consider the following polynomial, encoding the homological information of the embedding of a graph G in the torus, defined by the state sum

$$\tilde{P}_G(X, Y, W, A, B) := \sum_{H \subset G} (-1)^{E(G)-E(H)} X^{c(H)} Y^{n(H)} W^{\bar{c}(H)} A^{s(H)} B^{s^\perp(H)}, \tag{3.3}$$

where the summation is taken over all spanning subgraphs of G , $E(G)$ denotes the number of edges of G , and $(-1)^{E(G)-E(H)}$ provides a convenient normalization. Note that our convention for the sign and the variables differs from the usual convention for the Tutte polynomial. The usual proof (cf. [18, Lemma 2.2]) shows that this polynomial satisfies the contraction-deletion relation $\tilde{P}_G = \tilde{P}_{G/e} - \tilde{P}_{G \setminus e}$ for non-loop edges. (Note that, as in [18], the graphs $G, G/e, G \setminus e$ are considered as subsets of a fixed surface. Throughout this paper the surface is the torus \mathbb{T} .)

Remark. The polynomials defined in [6, 18] are specializations of \tilde{P} in the case of graphs embedded in the torus.

To establish a relation with the trace evaluation in TQFT, consider the specialization of \tilde{P} obtained by setting $X = B = 1$:

$$P_G(Y, W, A) := \sum_{H \subset G} (-1)^{E(G)-E(H)} Y^{n(H)} W^{\bar{c}(H)} A^{s(H)}. \tag{3.4}$$

This is a generalization of the flow polynomial, including variables W and A which reflect the topological information of how the graph G wraps around the torus. In particular, if G is homologically trivial on the torus (the rank $r(G \subset \mathbb{T})$ is zero), $P_G(Y, W, A)$ recovers the flow polynomial $F_G(Y)$. We thus name P_G the “topological flow polynomial.”

Three key examples are illustrated in Figure 6. For the graph consisting of k disjoint, trivial loops on the torus in Figure 6 (a), the polynomial $P = (Y - 1)^k$. For the

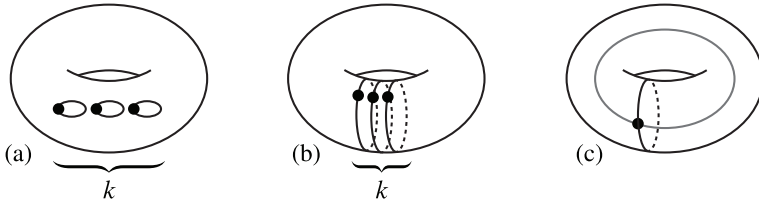
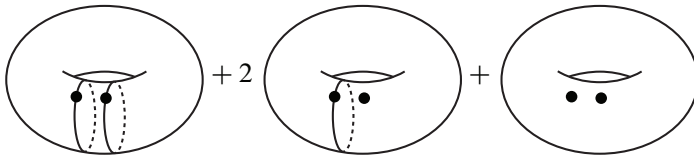


Figure 6

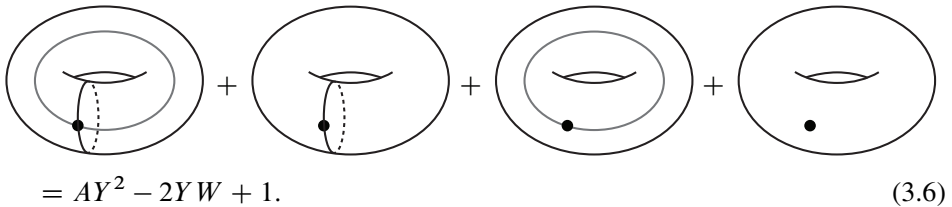
graph consisting of k non-trivial loops in Figure 6(b), $P = (YW - 1)^k$. The calculation is simple; for example the subgraphs H are



and so here the polynomial is

$$= Y^2W^2 - 2YW + 1 = (YW - 1)^2. \tag{3.5}$$

Finally, the polynomial of the graph in Figure 6(c) is computed as follows:



3.1. Duality

The chromatic and flow polynomials χ, F are 1-variable specializations of the Tutte polynomial, satisfying the relation $F_G(Q) = Q^{-1} \chi_{G^*}(Q)$, where G is a planar graph and G^* is its dual. We can extend this duality to the torus by defining the “topological chromatic polynomial.” Namely, we specialize \tilde{P}_G in (3.3) to

$$C_G(X, U, B) := \sum_{H \subset G} (-1)^{E(H)} X^{c(H)} U^{\tilde{c}(H)} B^{s^\perp(H)}. \tag{3.7}$$

When $r(H \subset \mathbb{T}) = 0$, $C_G(X, U, B)$ is the chromatic polynomial $\chi_G(X)$. Analogously to the proof of [18, Theorem 3.1], one shows that for a cellulation $G \subset \mathbb{T}$ (i.e., when

each face of the embedding is a 2-cell),

$$P_G(Y, W, A) = C_{G^*}(Y, YW, AY), \tag{3.8}$$

where $G^* \subset \mathbb{T}$ is the dual graph. This topological chromatic polynomial is thus dual to the topological flow polynomial P_G from (3.4).

4. TQFT trace as an evaluation of a graph polynomial

4.1. TQFT trace

Given an odd r and a multi-curve $\gamma \subset \mathbb{T}$, the trace of γ is defined as $Z_r(\mathbb{T} \times S^1, \gamma)$, the quantum invariant of the banded link γ in the 3-manifold $\mathbb{T} \times S^1$ [5, 1.2]. Concretely, it may be calculated as the trace of the curve operator in $\text{Hom}(V_r, V_r)$ with respect to the basis discussed in Section 2. This basis is given by the core circle of a fixed solid torus H , bounded by \mathbb{T} , labeled with an integer $0 \leq j \leq r - 2$. For a graph $G \subset \mathbb{T}$, the trace is defined by mapping G to a linear combination of multi-curves using Φ in (2.4) and then computing the trace of $\Phi(G)$.

While one could work with the full $\text{SU}(2)$ TQFT vector space V_r , the invariants of graphs obtained by putting the 2nd Jones–Wenzl projector on the edges, as in (2.4), naturally fit in the context of the $\text{SO}(3)$ theory. This corresponds to taking the subspace \bar{V}_r of V_r , spanned by even labels. For the remainder of the paper, $\text{tr}_r(G)$ will be evaluated as the trace of G considered as an operator in $\text{Hom}(\bar{V}_r, \bar{V}_r)$. A basis of \bar{V}_r is given by the core circle e_j of a solid torus bounded by \mathbb{T} , labeled with an even integer $0 \leq j \leq r - 2$. The result of G applied to a basis element e_j may be computed by pushing G (considered as a quantum spin network with edges labeled by 2) into the solid torus and re-expressing the result as a linear combination of $\{e_j\}$ using the recoupling theory [16]. In the examples below the trace will be computed using the expansion $\Phi(G)$ of G in terms of multi-curves; the multi-curves in question will act diagonally on \bar{V}_r with respect to the basis $\{e_j, 0 \leq j \leq r - 2, j \text{ even}\}$. We emphasize that while multi-curves (consisting of “spin 1/2 loops,” or in the usual TQFT terminology loops labelled 1) are elements of $\text{SU}(2)$ and not $\text{SO}(3)$ theory, the configurations of multi-loops considered below preserve the subspace \bar{V}_5 , and they provide a convenient evaluation method.

We give several sample calculations of the trace tr_5 , used in the proof below. First consider k trivial loops (labelled 1) on the torus. The usual d -isotopy relation states that removing a loop gives a factor $d = \phi$, so tr_5 equals ϕ^k times the trace of the empty diagram. Since the dimension of the space (spanned by the core of the solid torus with labels 0 and 2) is 2, the result is $2\phi^k$. The trace evaluation of the graph

consisting of k trivial loops (Figure 6 (a)) equals $2(d^2 - 1)^k$, which (precisely at this root of unity!) also equals $2\phi^k$.

Now, consider non-trivial (spin 1/2) loops on the torus in (4.1). Using (2.5), the action on \bar{V}_5 is seen to be diagonal:

$$\underbrace{\left(\text{torus with } k \text{ loops labeled } j \right)}_k = \left[\frac{\sin(2(j+1)\pi/5)}{\sin((j+1)\pi/5)} \right]^k \left(\text{torus with } j \text{ loops} \right), \quad j = 0, 2. \quad (4.1)$$

Therefore, the trace of k non-trivial loops with label 1 on the torus equals

$$\text{tr}_5 \left(\underbrace{\text{torus with } k \text{ loops}}_k \right) = \left[\frac{\sin(2\pi/5)}{\sin(\pi/5)} \right]^k + \left[\frac{\sin(6\pi/5)}{\sin(3\pi/5)} \right]^k = \phi^k + (-\phi^{-1})^k. \quad (4.2)$$

The analogous calculation for the *graph* consisting of k non-trivial loops on the torus (or “spin 1 loops”) gives

$$\underbrace{\left(\text{torus with } k \text{ loops} \right)}_k = \left[\frac{\sin(3\pi/5)}{\sin(\pi/5)} \right]^k + \left[\frac{\sin(9\pi/5)}{\sin(3\pi/5)} \right]^k = \phi^k + (-\phi^{-1})^k. \quad (4.3)$$

The answer is again the same as for spin 1/2 loops precisely at the 5th root of unity. Note that the $SO(3)$ trace is invariant under modular transformations of the torus, so (4.3) gives the trace of *any* k non-trivial, spin 1 loops on the torus. The situation is a bit more subtle with spin 1/2 loops: the calculations in (4.1), (4.2) work specifically for non-trivial loops which bound disks intersecting the core of the solid torus once. A single spin 1/2 loop which wraps in some other way around the torus and acts as a curve operator $V_5 \rightarrow V_5$, does not have to preserve the subspace \bar{V}_5 . Nevertheless, an *even* number of non-trivial curves preserve \bar{V}_5 , and moreover the evaluation (4.2) for k even is in fact modular invariant: using (2.4), a pair of parallel spin 1/2 loops may be expressed as a spin 1 loop plus a scalar multiple of a trivial loop. This property will be used in the following section to evaluate the trace of graphs on the torus in terms of surround loops.

Remark 4.2. There are two equivalent ways of computing the trace in (4.3): one using the formula (2.5) directly, or alternatively the 2nd JW projectors can be expanded into linear combinations of spin 1/2 loops, reducing the calculation to (4.2).

Finally, the trace of the graph in Figure 7 is obtained by expanding both second projectors, and applying (4.2).

$$\begin{aligned}
 \text{tr}_5 &= d \text{tr}_5 \\
 &= d \text{tr}_5 - \text{tr}_5 \\
 &\quad - \text{tr}_5 + \frac{1}{d} \text{tr}_5 \\
 &= 2\phi^2 - 2\left(\phi^2 + \left(\frac{1}{\phi}\right)^2\right) + 2 = 2 - \frac{2}{\phi^2}
 \end{aligned}$$

Figure 7. The factor d in the top line comes from the normalization of the map Φ (Figure 2.4). At the 5th root of unity $d = \phi$. Both first and last terms in the bottom line have a trivial loop, evaluating to d , and the factor 2 corresponds to the trace of the empty diagram. The two middle terms are evaluated according to (4.2).

4.3. Trace and graph evaluations

Definition 4.1. Given a graph $G \subset \mathbb{T}$, consider

$$R_5(G) := P_G(\phi^2, 1, \phi^{-2}) + P_G(\phi^2, \phi^{-4}, \phi^{-2}) \tag{4.4}$$

The two summands in the definition of $R_5(G)$ are given by evaluations of the polynomial P_G in (3.4). In both cases, $Y = \phi^2$ and $A = \phi^{-2}$. Note that the first summand corresponds to $YW = \phi^2$, and the second one to $YW = \phi^{-2}$.

Theorem 4.2. Given any graph $G \subset \mathbb{T}$, the $SO(3)$ TQFT trace evaluation $\text{tr}_5(G)$ equals $R_5(G)$.

This result is the TQFT version on the torus, at $Q = \phi + 1$ corresponding to $q = e^{2\pi i/5}$ (see (2.2)) of the loop evaluation of the flow polynomial of planar graphs. It is interesting to note that the loop evaluation in the planar case holds for any value of the parameter (cf. [11, Lemma 2.5]), while the statement on the torus makes sense only at roots of unity (Theorems 4.2, 4.4) where TQFTs are defined.

Proof of Theorem 4.2. We begin the proof by comparing calculations of $\text{tr}_5(G)$ and $R_5(G)$ for the graphs in Figure 6, using results of Sections 3 and 4.1.

(a) G consists of k trivial loops, Figure 6 (a).

$$\text{tr}_5(G) = 2(d^2 - 1)^k = 2\phi^k, \quad R_5(G) = (Y - 1)^k + (Y - 1)^k.$$

The factor 2 in the expression for $\text{tr}_5(G)$ comes from the dimension 2 of the vector space spanned by the even labels 0, 2. Since $Y = \phi^2$, the two expressions coincide.

(b) k non-trivial loops, Figure 6 (b). According to (4.3), $\text{tr}_5(G) = \phi^k + (-\phi^{-1})^k$. By (3.5), $R_5(G) = (YW - 1)^k|_{YW=\phi^2} + (YW - 1)^k|_{YW=\phi^{-2}}$. Individual terms match: $(\phi^2 - 1)^k + (\phi^{-2} - 1)^k = \phi^k + (-\phi^{-1})^k$.

(c) The graph in Figure 6 (c). The TQFT calculation in Figure 7 gives $\text{tr}_5(G) = 2\phi^2 - 2(\phi^2 + (\frac{1}{\phi})^2) + 2$. By (3.6), $P_G(Y, W, A) = AY^2 - 2YW + 1$. The two evaluations of P_G , contributing to $R_5(G)$, give $\phi^2 - 2\phi^2 + 1$ and $\phi^2 - 2(\frac{1}{\phi})^2 + 1$, adding up to the expression for $\text{tr}_5(G)$.

The proof of Theorem 4.2 for an arbitrary graph $G \subset \mathbb{T}$ is obtained by expanding the second JW projectors for all edges. The resulting summands for the TQFT trace are in 1-1 correspondence with spanning subgraph $H \subset G$. To be precise, given a spanning subgraph H , in this correspondence the first term in the expansion (2.4) of the 2nd projector is taken for each edge e in H , and the second term is taken for each edge e in $G \setminus H$. The resulting loop configuration, called the *surround loops*, is the boundary of a regular neighborhood of H on the surface. Each individual term in the trace evaluation equals the sum of two entries, corresponding to the two labels 0, 2, and we show next that these entries precisely match the corresponding terms in the expansions $P_G(\phi^2, 1, \phi^{-2}), P_G(\phi^2, \phi^{-4}, \phi^{-2})$.

For each spanning subgraph H there are three cases, analogous to the examples (a)–(c) above.

(A) H is homologically trivial on the torus: $H_1(H) \rightarrow H_1(\mathbb{T})$ is the zero map. The exponents of the variables W and A in (3.4) are zero in this case. The proof that loop evaluation in TQFT equals the summand in the definition of the graph polynomial (3.4) is thus identical to the planar case [11, Lemma 2.5]. Both quantities in the statement of the theorem have a factor 2: for $\text{tr}_5(G)$ this is because $\dim(\bar{V}_5) = 2$; for $R_5(G)$ the factor is the result of adding two identical summands in (4.4).

(\mathcal{B}) The image of $H_1(H) \rightarrow H_1(\mathbb{T})$ has rank 1. In this case $s(H) = 0$. Recall that $\bar{c}(H)$ denotes the number of connected components $H^{(i)}$ of H such that $H_1(H^{(i)}) \rightarrow H_1(\mathbb{T})$ of rank 1 for each i . The term in the expansion of $R_5(G)$ corresponding to H is

$$\begin{aligned} & (-1)^{E(G)-E(H)} \phi^{2n(H)} [1^{\bar{c}(H)} + \phi^{-4\bar{c}(H)}] \\ & = (-1)^{E(G)-E(H)} \phi^{2(n(H)-\bar{c}(H))} [\phi^{2\bar{c}(H)} + \phi^{-2\bar{c}(H)}]. \end{aligned}$$

Each $H^{(i)}$ has two surround loops which are non-trivial on the torus. In the calculation of $\text{tr}_5(G)$, these $\bar{c}(H)$ non-trivial loops give a factor $\phi^{2\bar{c}(H)} + \phi^{-2\bar{c}(H)}$, matching the factor in square brackets in the calculation of $R_5(G)$ above.

The last step is to check that the remaining factor $(-1)^{E(G)-E(H)} \phi^{2(n(H)-\bar{c}(H))}$ above corresponds to the normalization and the trivial surround loops in the trace evaluation. As explained after (2.4), the normalization factor in the definition of Φ is $d^{E(G)-V(G)}$. Moreover, each edge in $G \setminus H$ gives rise to an additional factor $-d^{-1}$ coming from the second term of the JW projector. This gives the desired sign $(-1)^{E(G)-E(H)}$. Thus, the overall normalization factor corresponding to H is $d^{E(H)-V(H)}$, where $d = \phi$. In addition, each trivial surround loop of H gives a factor ϕ in the trace evaluation. An Euler characteristic count gives the equality

$$E(H) - V(H) + \text{number of trivial loops} = 2(n(H) - \bar{c}(H)),$$

concluding the proof in case \mathcal{B} .

(\mathcal{C}) $H_1(H) \rightarrow H_1(\mathbb{T})$ is surjective, so $s(H) = 1$ and $\bar{c}(H) = 0$. This case is similar to (\mathcal{A}) since all surround loops are trivial on the torus. Because of the homological assumption, there are two fewer surround loops than in the planar case, expected from the nullity $n(H)$. In the TQFT evaluation this undercount gives a factor d^{-2} . This factor precisely matches the factor $A^{s(H)} = A = \phi^{-2}$ in (3.4). ■

Recall that the vanishing of the Jones–Wenzl projector is built into the definition of the TQFT vector space at the corresponding root of unity, so the 4-th JW projector gives a local relation in \bar{V}_5 .

Corollary 4.3. *The graph evaluation $R_5(G)$ satisfies the local relation (2.6), corresponding to the 4-th Jones–Wenzl projector. More precisely, given three graphs G_X, G_I, G_E on the torus, locally related as shown in (2.6),*

$$\phi R_5(G_X) = R_5(G_I) + R_5(G_E).$$

More generally, given $G \subset \mathbb{T}$ and odd r , consider

$$R_r(G) := \sum_{j=0, j \text{ even}}^{r-2} P_G(d^2, W_{j,r}, d^{-2}), \tag{4.5}$$

where $d = q^{1/2} + q^{-1/2}$ is the TQFT loop value corresponding to the root of unity $q = e^{2\pi i/r}$, and $W_{j,r}$ is defined by

$$Y W_{j,r} - 1 = \frac{\sin(2(j + 1)\pi/r)}{\sin((j + 1)\pi/r)}.$$

The proof of the following result is directly analogous to that of Theorem 4.2, with TQFT sectors precisely corresponding to the summands in (4.5):

Theorem 4.4. *The SO(3) TQFT trace evaluation of G at $q = e^{2\pi i/r}$ equals $R_r(G)$.*

Remark 4.4. A generalization of the polynomial P for links L in $\mathbb{T} \times [0, 1]$ (along the lines of [18, Section 6]) gives a similar expression for the SU(2) trace of L . A polynomial P_L for more general links in a surface Σ times the circle was formulated in [19]. It is an interesting question whether the polynomial of [19] can be defined for ribbon graphs in $\Sigma \times S^1$, and whether our results extend to this setting.

5. Golden identity for graphs on the torus

Using TQFT methods developed above, in this section we formulate and prove an extension of the Tutte golden identity for graphs on the torus.

5.1. Proof of the Tutte golden identity (1.1) for planar graphs

We start by summarizing the ideas underlying the proof in the planar case. Following [11], we prove here the golden identity for the flow polynomial of cubic planar graphs G : $F_G(\phi + 2) = \phi^E (F_G(\phi + 1))^2$. The version of the contraction-deletion rule for cubic graphs reads

$$\text{Diagram 1} + \text{Diagram 2} = \text{Diagram 3} + \text{Diagram 4}. \tag{5.1}$$

Using induction on the number of edges, it suffices to show that if three of the graphs in (5.1) for $F_G(\phi + 2)$ satisfy the golden identity, then the fourth one does as well. Given a cubic graph G , consider $\phi^E (F_G(\phi + 1))^2$. It is convenient to formally depict, as in (5.2), two identical copies of G , each one evaluated at $\phi + 1$, with an overall factor $\phi^E = \phi^{3V/2}$.

$$\text{Diagram 1} \xrightarrow{\Psi} \phi^{3/2} \text{Diagram 2} \quad \text{Diagram 3} \xrightarrow{\Psi} \phi^3 \text{Diagram 4}. \tag{5.2}$$

Here E and V denote the number of edges and vertices, respectively, of G . This doubling of lines is *not* that in the map Φ using the projector p_2 , but rather it indicates that the map Ψ takes G to the pair (G, G) . Note that for $G = \text{circle}$, $F_{\text{circle}}(\phi + 2) = \phi + 1$. The corresponding value for $\Psi(\text{circle})$ is $\phi^2 = \phi + 1$, indeed the same.

The strategy is to check that the evaluation $\phi^E (F_G(\phi + 1))^2$ satisfies the relation (5.1) as a consequence of the *additional* local relation at $Q = \phi + 1$. This additional relation is the graph version (2.6) of the 4th Jones–Wenzl projector. Using the contraction-deletion rule, one checks that (2.6) is equivalent to each of the two relations shown in Figure 8.

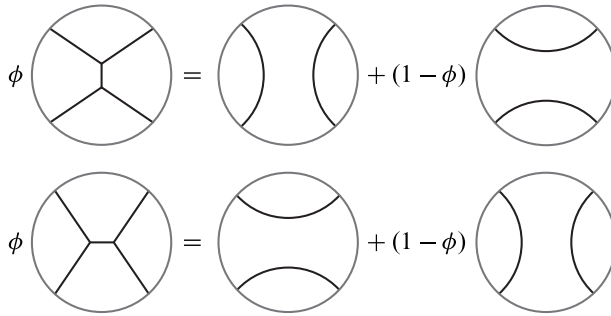


Figure 8. Local relations for the flow polynomial at $Q = \phi + 1$, equivalent to Tutte’s relation (2.6).

Consider the image of (5.1) under Ψ :

$$\phi^3 \cdot \left(\begin{array}{c} \text{Y-junction} \\ \text{with dashed lines} \end{array} \right) + \left(\begin{array}{c} \text{Two arcs} \\ \text{on a circle} \end{array} \right) = \phi^3 \cdot \left(\begin{array}{c} \text{X-junction} \\ \text{with dashed lines} \end{array} \right) + \left(\begin{array}{c} \text{Two arcs} \\ \text{on a circle} \end{array} \right). \quad (5.3)$$

Applying the relation on the left in Figure 8 to both copies of the graph on the left in (5.3) yields Figure 9. The resulting expression on the right is invariant under 90 degree rotation, so must also be equal to the graph on the right of (5.3). Thus, (5.3) holds, showing that the evaluation $\phi^E (F_G(\phi + 1))^2$ satisfies the contraction-deletion relation (5.1). This concludes the proof of the golden identity for the flow polynomial of planar cubic graphs.

5.2. Extension to graphs on the torus

The expression (4.5) is defined for odd r . We generalize it with the following sum of evaluations of the graph polynomial P_G in (3.4):

$$R_{10}(G) := P_G(Y, W_1, A) + P_G(Y, W_2, A) + 2P_G(Y, W_3, A), \quad (5.4)$$

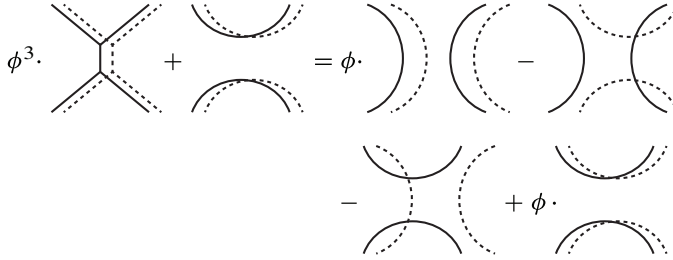


Figure 9

where $Y = \phi + 2$, $A = (2(\phi + 2))^{-1}$, and the values W_j , $j = 1, 2, 3$, are defined by

$$Y W_1 = \phi + 2, \quad Y W_2 = 1 + \phi^{-2}, \quad Y W_3 = 0.$$

The choice of these values may be thought of as a choice of particular sectors of the $SO(3)$ TQFT vector space of the torus at $q = e^{2\pi i/10}$. (Our forthcoming work, relating these results to lattice models on the torus, will give further evidence for why this is a relevant invariant at this root of unity.) The value of $R_{10}(G)$ for G a trivial loop on the torus equals $4(Y - 1) = 4\phi^2$. Using (3.5), the value of $R_{10}(G)$ for the graph consisting of a single non-trivial loop is seen to be $\phi^2 + \phi^{-2} - 2$.

We are in a position to state the main result of this section.

Theorem 5.1. *Let $G \subset \mathbb{T}$ be a cubic graph. Then*

$$R_{10}(G) = \phi^E R_5(G)^2, \tag{5.5}$$

where E is the number of edges of G .

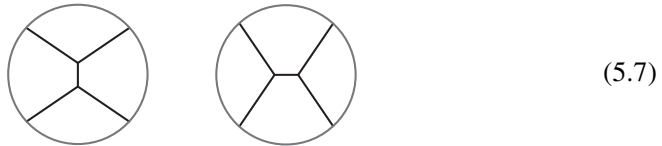
Proof. As usual, we allow cubic graphs with disjoint loops; such loops do not count towards E . The version of the contraction-deletion relation for cubic graphs is shown in (5.1). The proof in the planar case (see Section 5.1) showed that if three of the graphs in (5.1) satisfy the golden identity, then the fourth one satisfies it as well. This fact holds for the identity (5.5) for graphs on the torus as well. Indeed, (5.1) holds for $R_{10}(G)$ since it is defined as the sum (5.4) of polynomials satisfying the contraction-deletion rule. And (5.1) holds for $\phi^E R_5(G)^2$ for the same reason as in Section 5.1, since by Corollary 4.3 $R_5(G)$ obeys the local relation corresponding to the 4th JW projector.

For cubic graphs G which are homologically trivial on the torus ($r(G \subset \mathbb{T}) = 0$ in the notation of Section 3), the proof of (5.5) follows from the planar case in Section 5.1 since the polynomial P_G in (3.4) equals the flow polynomial F_G . (For example, calculations in Section 3 show that in the special case of the graph consisting of k trivial loops, $R_5(G) = 2\phi^k$, and $R_{10}(G) = 4\phi^{2k} = R_5(G)^2$.)

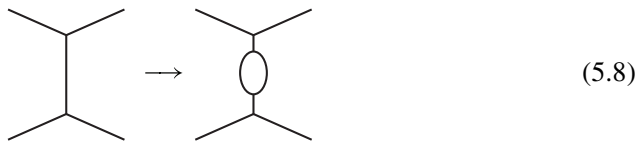
Next, consider the case of cubic graphs G of rank $r(G \subset \mathbb{T}) = 2$. Consider a minimal cubic graph G of this type, shown in (5.6), where the square with opposite sides identified is the usual representation of the torus. A direct calculation using (3.4), or alternatively using the contraction-deletion rule to reduce this to calculations above, shows $R_5(G) = R_{10}(G) = \phi^{-3}$, proving (5.5) in this case:



The proof in general for rank 2 cubic graphs is by induction on the number of edges. It is proved in [9] that any two triangulations of the torus with the same number of vertices are related by diagonal flips, up to equivalence given by diffeomorphisms. (This was extended in [22] to pseudo-triangulations of surfaces of any genus, where an embedding $\Gamma \subset \mathbb{T}$ is a *pseudo-triangulation* if each face is a three-edged 2-cell, possibly with multiple edges and loops.) Formulated in terms of dual cubic graphs, two cellular embeddings of cubic graphs (or in other words rank 2 graphs) on the torus are related by the $I - H$ move:



The relation (5.1) accomplishes the $I - H$ move, while also introducing graphs with fewer edges. The theorem has been checked for a minimal cubic graph in (5.6), and the inductive step is achieved by a local modification (5.8), which increases the number of edges and preserves (5.5):



Finally, consider cubic graphs of rank 1 (that is, $r(G \subset \mathbb{T}) = 1$), or equivalently graphs on the cylinder. The fact that triangulations of the sphere with the same number of vertices are related by diagonal flips dates back to [27]. Using (5.1) and (5.8) as above, the proof in the rank 1 case therefore follows from the calculation for G consisting of k non-trivial loops on the torus. In this case, using (3.5) one has $R_5(G) = \phi^k + (-\phi^{-1})^k$ and $R_{10}(G) = \phi^{2k} + \phi^{-2k} + 2(-1)^k = R_5(G)^2$. ■

Remark 5.3. Theorem 5.1 is an extension of the golden identity for the flow polynomial of planar cubic graphs. The focus of this paper is on the “topological flow

polynomial” P_G , since it is related to the TQFT trace evaluation, as stated in Theorem 4.4. It is worth noting that an analogue of the invariants $R_5(G)$, $R_{10}(G)$ may be defined using the polynomial C_G in place of P_G . Using the duality relation (3.8), the identity (5.5) then gives rise to an extension of the original Tutte golden identity (1.1) for the “topological chromatic polynomial” C_G of triangulations of the torus.

Acknowledgments. Vyacheslav Krushkal would like to thank both Calvin McPhail-Snyder and Sittipong Thamrongpaioj for discussions about polynomial invariants of graphs on surfaces. He also would like to thank All Souls College and the Department of Physics at the University of Oxford for hospitality and support. The authors would like to thank the anonymous referees for their comments which improved the paper.

Funding. Vyacheslav Krushkal was supported in part by NSF grant DMS-1612159.

References

- [1] D. Aasen, P. Fendley, and R. S. K. Mong, Topological defects on the lattice: Dualities and degeneracies. 2020, arXiv:2008.08598
- [2] D. Aasen, R. S. K. Mong, and P. Fendley, Topological defects on the lattice: I. The Ising model. *J. Phys. A* **49** (2016), no. 35, article id. 354001 Zbl 1353.82011 MR 3543452
- [3] I. Agol and V. Krushkal, Tutte relations, TQFT, and planarity of cubic graphs. *Illinois J. Math.* **60** (2016), no. 1, 273–288 Zbl 1365.05137 MR 3665181
- [4] I. Agol and V. Krushkal, Structure of the flow and Yamada polynomials of cubic graphs. In *Breadth in contemporary topology*, pp. 1–20, Proc. Sympos. Pure Math. 102, American Mathematical Society, Providence, R.I., 2019 Zbl 1453.05051 MR 3967356
- [5] C. Blanchet, N. Habegger, G. Masbaum, and P. Vogel, Topological quantum field theories derived from the Kauffman bracket. *Topology* **34** (1995), no. 4, 883–927 Zbl 0887.57009 MR 1362791
- [6] B. Bollobás and O. Riordan, A polynomial of graphs on surfaces. *Math. Ann.* **323** (2002), no. 1, 81–96 Zbl 1004.05021 MR 1906909
- [7] D. Cimasoni and N. Reshetikhin, Dimers on surface graphs and spin structures. I. *Comm. Math. Phys.* **275** (2007), no. 1, 187–208 Zbl 1135.82006 MR 2335773
- [8] O. T. Dasbach, D. Futer, E. Kalfagianni, X.-S. Lin, and N. W. Stoltzfus, The Jones polynomial and graphs on surfaces. *J. Combin. Theory Ser. B* **98** (2008), no. 2, 384–399 Zbl 1135.05015 MR 2389605
- [9] A. K. Dewdney, Wagner’s theorem for torus graphs. *Discrete Math.* **4** (1973), 139–149 Zbl 0249.05109 MR 309773
- [10] P. Di Francesco, H. Saleur, and J.-B. Zuber, Relations between the Coulomb gas picture and conformal invariance of two-dimensional critical models. *J. Statist. Phys.* **49** (1987), no. 1-2, 57–79 Zbl 0960.82507 MR 923852

- [11] P. Fendley and V. Krushkal, Tutte chromatic identities from the Temperley–Lieb algebra. *Geom. Topol.* **13** (2009), no. 2, 709–741 Zbl [1184.57002](#) MR [2469528](#)
- [12] P. Fendley and V. Krushkal, Link invariants, the chromatic polynomial and the Potts model. *Adv. Theor. Math. Phys.* **14** (2010), no. 2, 507–540 Zbl [1207.82007](#) MR [2721654](#)
- [13] P. Fendley and V. Krushkal, Loop models and a topological Tutte polynomial for graphs on the torus. In preparation
- [14] M. Freedman, C. Nayak, K. Walker, and Z. Wang, On picture $(2 + 1)$ -TQFTs. In *Topology and physics*, pp. 19–106, Nankai Tracts Math. 12, World Scientific, Hackensack, N.J., 2008 Zbl [1168.81024](#) MR [2503392](#)
- [15] V. F. R. Jones, *Subfactors and knots*. CBMS Regional Reg. Conf. Ser. Math. 80, American Mathematical Society, Providence, R.I., 1991 Zbl [0743.46058](#) MR [1134131](#)
- [16] L. H. Kauffman and S. L. Lins, *Temperley–Lieb recoupling theory and invariants of 3-manifolds*. Ann. Math. Stud. 134, Princeton University Press, Princeton, N.J., 1994 Zbl [0821.57003](#) MR [1280463](#)
- [17] T. Krajewski, V. Rivasseau, A. Tanasă, and Z. Wang, Topological graph polynomials and quantum field theory. I. Heat kernel theories. *J. Noncommut. Geom.* **4** (2010), no. 1, 29–82 Zbl [1186.81095](#) MR [2575389](#)
- [18] V. Krushkal, Graphs, links, and duality on surfaces. *Combin. Probab. Comput.* **20** (2011), no. 2, 267–287 Zbl [1211.05029](#) MR [2769192](#)
- [19] J. Marché and R. Santharoubane, Asymptotics of quantum representations of surface groups. *Ann. Sci. Éc. Norm. Supér. (4)* **54** (2021), no. 5, 1275–1296 Zbl [1490.57009](#) MR [4363245](#)
- [20] C. McPhail-Snyder and K. A. Miller, Planar diagrams for local invariants of graphs in surfaces. *J. Knot Theory Ramifications* **29** (2020), no. 1, article id. 1950093 Zbl [1435.05111](#) MR [4079619](#)
- [21] S. Morrison, E. Peters, and N. Snyder, Knot polynomial identities and quantum group coincidences. *Quantum Topol.* **2** (2011), no. 2, 101–156 Zbl [1239.57031](#) MR [2783128](#)
- [22] S. Negami, Diagonal flips in pseudo-triangulations on closed surfaces. *Discrete Math.* **240** (2001), no. 1-3, 187–196 Zbl [0988.05033](#) MR [1855053](#)
- [23] V. Pasquier, Lattice derivation of modular invariant partition functions on the torus. *J. Phys. A* **20** (1987), no. 18, L1229–L1237 MR [926363](#)
- [24] H. N. V. Temperley and E. H. Lieb, Relations between the “percolation” and “colouring” problem and other graph-theoretical problems associated with regular planar lattices: some exact results for the “percolation” problem. *Proc. Roy. Soc. London Ser. A* **322** (1971), no. 1549, 251–280 Zbl [0211.56703](#) MR [498284](#)
- [25] W. T. Tutte, More about chromatic polynomials and the golden ratio. In *Combinatorial Structures and their Applications (Proc. Calgary Internat. Conf., Calgary, Alta., 1969)*, pp. 439–453, Gordon and Breach, New York, 1970 MR [0263698](#)
- [26] W. T. Tutte, On chromatic polynomials and the golden ratio. *J. Combinatorial Theory* **9** (1970), 289–296 Zbl [0209.55001](#) MR [272676](#)
- [27] K. Wagner, Bemerkungen zum Vierfarbenproblem. *Jahresber. Dtsch. Math.-Ver.* **46** (1936), 26–32

- [28] H. Wenzl, On sequences of projections. *C. R. Math. Rep. Acad. Sci. Canada* **9** (1987), no. 1, 5–9 Zbl [0622.47019](#) MR [873400](#)

Communicated by Joanna A. Ellis-Monaghan

Received 24 January 2020; revised 11 June 2021.

Paul Fendley

All Souls College and Rudolf Peierls Centre for Theoretical Physics, Parks Rd,
Oxford OX1 3PU, United Kingdom; paul.fendley@physics.ox.ac.uk

Vyacheslav Krushkal

Department of Mathematics, University of Virginia, Charlottesville, VA 22904-4137, USA;
krushkal@virginia.edu